Accepted Manuscript

Discovery of 3-(4-sulfamoylnaphthyl)pyrazolo[1,5-a]pyrimidines as potent and selective ALK2 inhibitors

Jian-kang Jiang, Xiuli Huang, Khalida Shamim, Paresma R. Patel, Arthur Lee, Amy Q. Wang, Kimloan Nguyen, Gregory Tawa, Gregory D. Cuny, Paul B. Yu, Wei Zheng, Xin Xu, Philip Sanderson, Wenwei Huang

Please cite this article as: Jiang, J-k., Huang, X., Shamim, K., Patel, P.R., Lee, A., Wang, A.Q., Nguyen, K., Tawa, G., Cuny, G.D., Yu, P.B., Zheng, W., Xu, X., Sanderson, P., Huang, W., Discovery of 3-(4-sulfamoylnaphthyl)pyrazolo[1,5-a]pyrimidines as potent and selective ALK2 inhibitors, *Bioorganic & Medicinal Chemistry Letters* (2018), doi: https://doi.org/10.1016/j.bmcl.2018.09.006
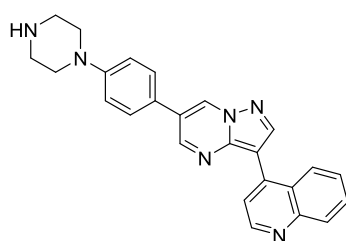
Graphical Abstract

Discovery of 3-(4-sulfamoylnaphthyl)pyrazolo[1,5-a]pyrimidines as potent and selective ALK2 inhibitors

Jian-kang Jiang[a,*], Xiuli Huang[a], Khalida Shamim[a], Paresma R. Patel[a], Arthur Lee[a], Amy Q. Wang[a], Kimloan Nguyen[a], Gregory Tawa[a], Gregory D. Cuny[b], Paul B. Yu[c], Wei Zheng[a], Xin Xu[a], Philip Sanderson[a] and Wenwei Huang[a,*]

LDN193189

IC_{50}= 17 nM for ALK2;
IC_{50}= 19 nM for ALK3;
No ALK2/ALK3 selectivity.

23

IC_{50}= 9 nM for ALK2;
IC_{50}= 6439 nM for ALK3;
ALK2/ALK3 selectivity: >700-fold.
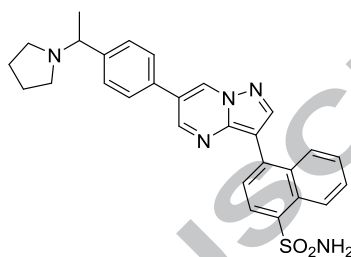
Discovery of 3-(4-sulfamoylnaphthyl)pyrazolo[1,5-a]pyrimidines as potent and selective ALK2 inhibitors

Jian-kang Jiang[a,*], Xiuli Huang[a], Khalida Shamim[a], Paresma R. Patel[a], Arthur Lee[a], Amy Q. Wang[a], Kimloan Nguyen[a], Gregory Tawa[a], Gregory D. Cuny[b], Paul B. Yu[c], Wei Zheng[a], Xin Xu[a], Philip Sanderson[a] and Wenwei Huang[a,*]

[a] *National Center for Advancing Translational Sciences, National Institutes of Health, 9800 Medical Center Drive, Bethesda, Maryland, 20892-3370, USA*

[b] *Department of Pharmacological and Pharmaceutical Sciences, University of Houston, 4849 Calhoun Road, Health Building 2, Room 7036, Houston, Texas 77204, USA*

[c] *Brigham and Women's Hospital and Harvard Medical School, Division of Cardiovascular Medicine, 20 Shattuck Street, Thorn Biosciences 1219, Boston, Massachusetts 02115, USA*

Corresponding authors: 9800 Medical Center Drive, Rockville MD, USA, 20892; Email address: jiankangj@mail.nih.gov; Tel.: 1-301-827-7165 (J. K. Jiang) or Email address: huangwe@mail.nih.gov; Tel. 1-301-827-7164 (W. Huang).

ARTICLE INFO

ABSTRACT

The pyrazolo[1,5-a]pyrimidine LDN-193189 is a potent inhibitor of activin receptor-like kinase 2 (ALK2) but is nonselective for highly homologous ALK3 and shows only modest kinome selectivity. Herein, we describe the discovery of a novel series of potent and selective ALK2 inhibitors by replacing the quinolinyl with a 4-(sulfamoyl)naphthyl, yielding ALK2 inhibitors that exhibit not only excellent discrimination versus ALK3 but also high kinome selectivity. In addition, the optimized compound **23** demonstrates good ADME and in vivo pharmacokinetic properties.

2018 Elsevier Ltd. All rights reserved.

Fibrodysplasia ossificans progressiva (FOP) is an extremely rare and devastating disease that affects one per two million of the population at any time.[1-2] Although normal at birth except for deformed hallux, FOP patients develop heterotopic ossification (HO) of muscles, fascia and connective tissues induced by postnatal trauma, injury or inflammation, resulting in severe immobility and shortened life expectancy.[3-4] Genetic sequence analysis found >96% of FOP patients harbor an arginine to histidine mutation near the glycine-serine (GS) rich domain (c.617G>A; p.R206H) of *ACVR1* gene encoding ALK2,[5] one of seven bone morphogenetic protein (BMP) type 1 receptor kinases (ALK1-7). While ALK2 is typically thought to transduce BMP ligand signaling via phosphorylation of downstream SMAD effectors 1/5/8, recent investigations found that the $ALK2^{R206H}$ mutant gains responsiveness to activin A, resulting in dysregulated phosphorylation of SMAD1/5/8 and ultimately, the ectopic formation of endochondral bone.[6-7]

2

Current treatments for FOP are limited to corticosteroids and non-steroidal anti-inflammatory drugs for symptomatic relief and bisphosphonates during acute flares. However, none of these interventions have been demonstrated to prevent the formation of HO, or modify the natural course of disease. Several drug candidates for inhibiting the formation of HO by diverse mechanisms of action are in various stages of clinical development including an activin A neutralizing antibody,[8] a selective RAR-γ agonist (palovarotene)[9] and more recently the immunosuppressive agent rapamycin.[10-11] These strategies, while promising, have yet to demonstrate efficacy in human randomized clinical trials for FOP. They are not known to modify disease progression and have distinct side effect profiles, which may or may not limit their use in the target population. Thus, FOP remains a significant unmet medical need. Several chemotypes of ALK2 inhibitors have been reported[12-23] including LDN-193189 and K02288 (Figure 1). However, kinome-wide profiling showed LDN-193189 has only modest selectivity with no discrimination for ALK3.[16] With this in mind, we initiated medicinal chemistry efforts to identify novel next-generation ALK2 inhibitors with improved selectivity over ALK3 as compared to published tool compounds.
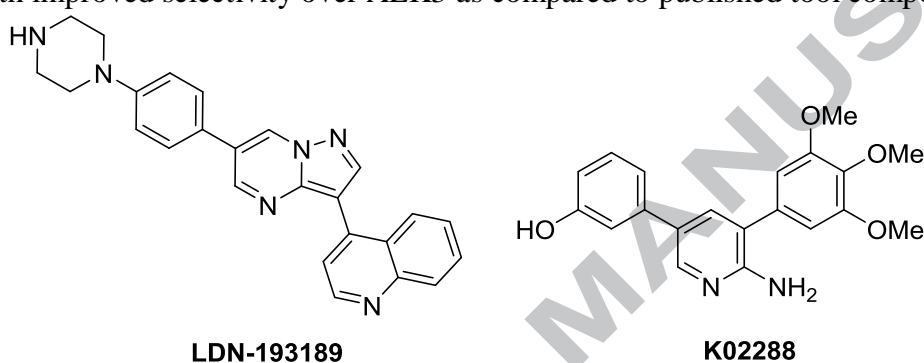

Figure 1. Structures of LDN-193189 and K02288

ALK2 and ALK3 share approximately 63% sequence homology in their kinase domains. The crystal structure of LDN-193189 bound to ALK2 (PDB: 3Q4U) indicates that the nitrogen of the quinolinyl ring forms a critical water-mediated hydrogen bond with the carboxyl side-chain of Glu248, which is conserved in BMP type 1 receptors including ALK3. Therefore, we envisioned replacing the quinolinyl moiety at the 3-position of the pyrazolo[1,5-a]pyrimidine core with other aromatics to exploit subtle differences in these regions of ALK2 and ALK3 in order to achieve better selectivity.

In addition to targeting the quinolinyl moiety, introduction of steric hindrance to the solvent exposed piperazine ring was pursued in order to reduce potential CYP450-mediated dealkylation of this group. This metabolic pathway was observed for LDN-193189 (unpublished data) which results in formation of the corresponding aniline (a potential genotoxin). Therefore, the initial set of designed derivatives utilized *cis*-2,6-dimethylpiperazine as the solvent exposed group and different aromatic moieties at the 3-position of the pyrazolo[1,5-a]pyrimidine core. Compounds **1-11** were prepared as shown in Scheme 1. Reaction of malonaldehyde **24** and pyrazole-5-amine (**25**) gave pyrazolopyrimidine **26** in 81% yield. Bromide **29** was prepared through a Pd₂(dba)₃/*t*-Bu₃PH⁺BF₄⁻ catalyzed Buchwald-Hartwig amination of **26** followed by treatment with *N*-bromosuccinamide (NBS). With **26** in hand, compound **1-11** were synthesized by using Suzuki-

3

Miyaura coupling reactions with either aryl boronic acids or aryl pinacol boronic esters followed by removal of the Boc protecting group with acid.
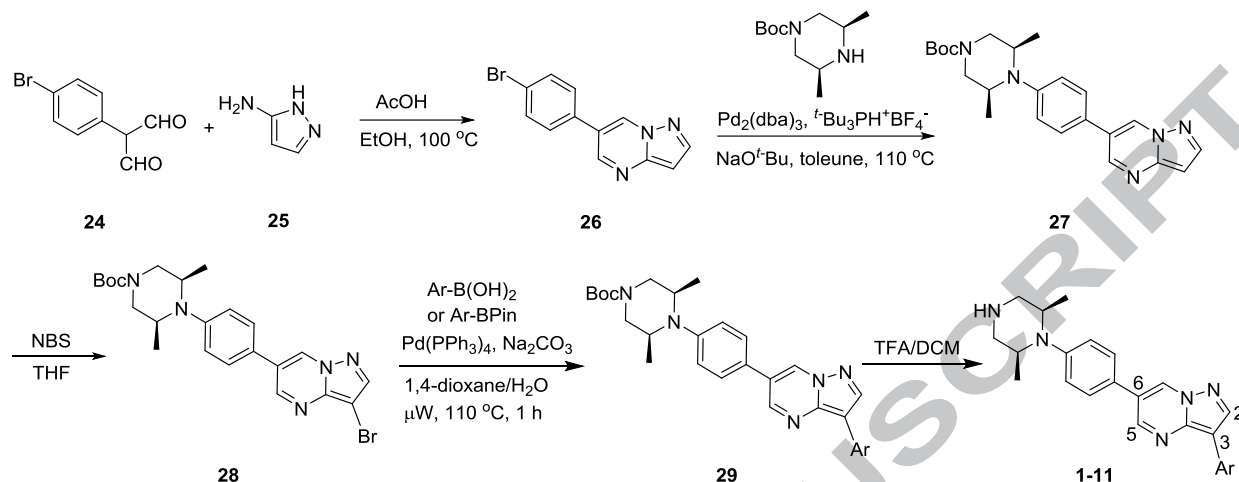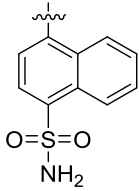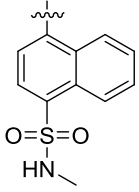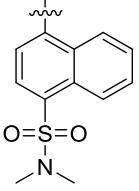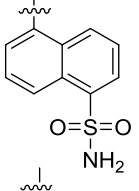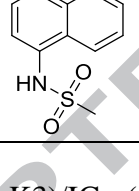

Scheme 1. The synthesis of analogs **1-11**; Pin=pinacol.

As depicted in Table 1, introduction of the *cis*-2,6-dimethylpiperazine in compound **1** retained potent ALK2 and ALK3 enzyme inhibitory activity (IC_{50}= 9 nM and 7 nM for ALK2 and ALK3, respectively). However, replacing the quinolinyl moiety with 4-(methylsulfonyl)phenyl (compound **2**) resulted in a significantly weaker ALK2 inhibitor (IC_{50}= ~2 μM). Interestingly, for derivative **3** with a 4-(sulfamoyl)phenyl group in the place of the quinolinyl, the potency for ALK2 inhibition improved ~4-fold (IC_{50}= 526 nM) compared to **2**. Adding either a methyl (compound **4**) or an amino (compound **5**) at the *ortho* position of the 4-sulfamoyl improved the ALK2 inhibitory activity by ~2-fold over **3**. Shifting the sulfamoyl group from the 4- to 3-position (compound **6**) improved ALK2 inhibitory activity another 2-fold. To our delight, **7**, with a 4-(sulfamoyl)naphthyl moiety at the 3-position of pyrazolo[1,5-a]pyrimidine core, showed markedly improved ALK2 inhibitory activity (IC_{50}= 19 nM) and excellent selectivity against ALK3. However, mono and di *N*–methylation of the $S(O)_2NH_2$ group proved detrimental for ALK2 potency as shown by analogs **8** and **9**, suggesting that the unsubstituted sulfamoyl might be critical for binding and well-accommodated in the active site of the enzyme. Shifting the sulfamoyl group from the 4- to 5-position on the naphthyl ring (compound **10**) led to ~3-fold decreased potency compared to **3** and its selectivity against ALK3 also decreased. Replacing the 4-sulfamoyl with a 4-methylsulfonamido group also resulted in significantly decreased ALK2 inhibitory activity as demonstrated by **11**.

Table 1. ALK2 and ALK3 inhibitory activity of **1**-**11**, which contain various groups at the 3-position of the pyrazolo[1,5-a]pyrimidine.
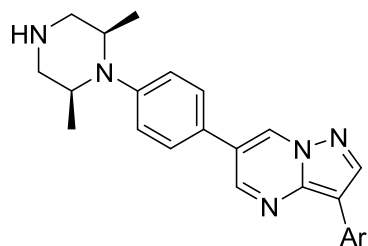
Compd	Ar	ALK2 (IC$_{50}$, nM)	ALK3 (IC$_{50}$, nM)	Selectivity (-fold)
LDN-193189		17	19	1.0
1		9	7	0.8
2		1971	>10,000	NA
3		526	ND	NA
4		246	16550	67.3
5		291	>10,000	NA
6		109	2534	23.2

5

7		19	3466	182.4
8		326	>10,000	NA
9		5990	64750	10.8
10		54	444	8.2
11		796	8897	11.2

*Selectivity= IC$_{50}$ (ALK3)/IC$_{50}$ (ALK2); **NA= not available; ***ND= not determined.

Based on the initial SAR, we identified a new ALK2 inhibitor (**7**) with a 4-(sulfamoyl)naphthyl ring attached to the pyrazolo[1,5-a]pyrimidine core that exhibited potent ALK2 potency and excellent selectivity for ALK2 versus ALK3. We constructed a computational model of the binding mode of **7** with ALK2 based on the reported co-crystal structure of LDN-193189 and ALK2 (Figure 2). The model revealed similar interactions and conformations at the hinge and the solvent-exposed region of ALK2.[24] However, the oxygen atoms of the 4-sulfamoyl group forms two direct hydrogen bonds with the enzyme, one with the amino side-chain of Lys235 and the other with the backbone amide NH of Asp354. We also generated a homology model of ALK3 using the ALK2 structure as a template. Compound **7** was then modeled into the ALK3 homology model binding pocket. Although both Lys235 and Asp354 are conserved in ALK2 and ALK3 enzymes, the sulfonamides were generally less potent against ALK3. The potency difference probably stems from the fact that the hinge residues of ALK3 are different than for ALK2. In particular, there is a histidine pair in ALK2 (His286 and His284) which in ALK3 is replaced by a His312 and Asp310 pair. When binding to ALK2 compound **7** forms a hydrogen bond with the

6

backbone nitrogen of His286 and the imidazole of His286 forms an edge on Pi stack interaction with His284. In the case of ALK3 however, His 312's histidine forms a hydrogen bond with the carboxylate of Asp310. This hydrogen bond pulls His312 towards Asp310 causing a puckered confirmation that pulls the hinge away from the ligand. We speculate that this reduces the ability of the pyrazolo-pyrimidine core to form a hydrogen bond with His312 in ALK3's hinge making compound **7** less potent against ALK3, Figure 3. Also, this computational model seems to explain the potency difference observed between compounds **7** and **9** against ALK2. As per model, the potency difference might arise due to the clash that the compound **9** methyl groups has with the back-end of the ALK2 pocket (Shown in Supporting information, Figure 1B). This steric clash does not exist for compound **7** which has hydrogen atoms in those positions (Shown in Supporting information, Figure 2A).
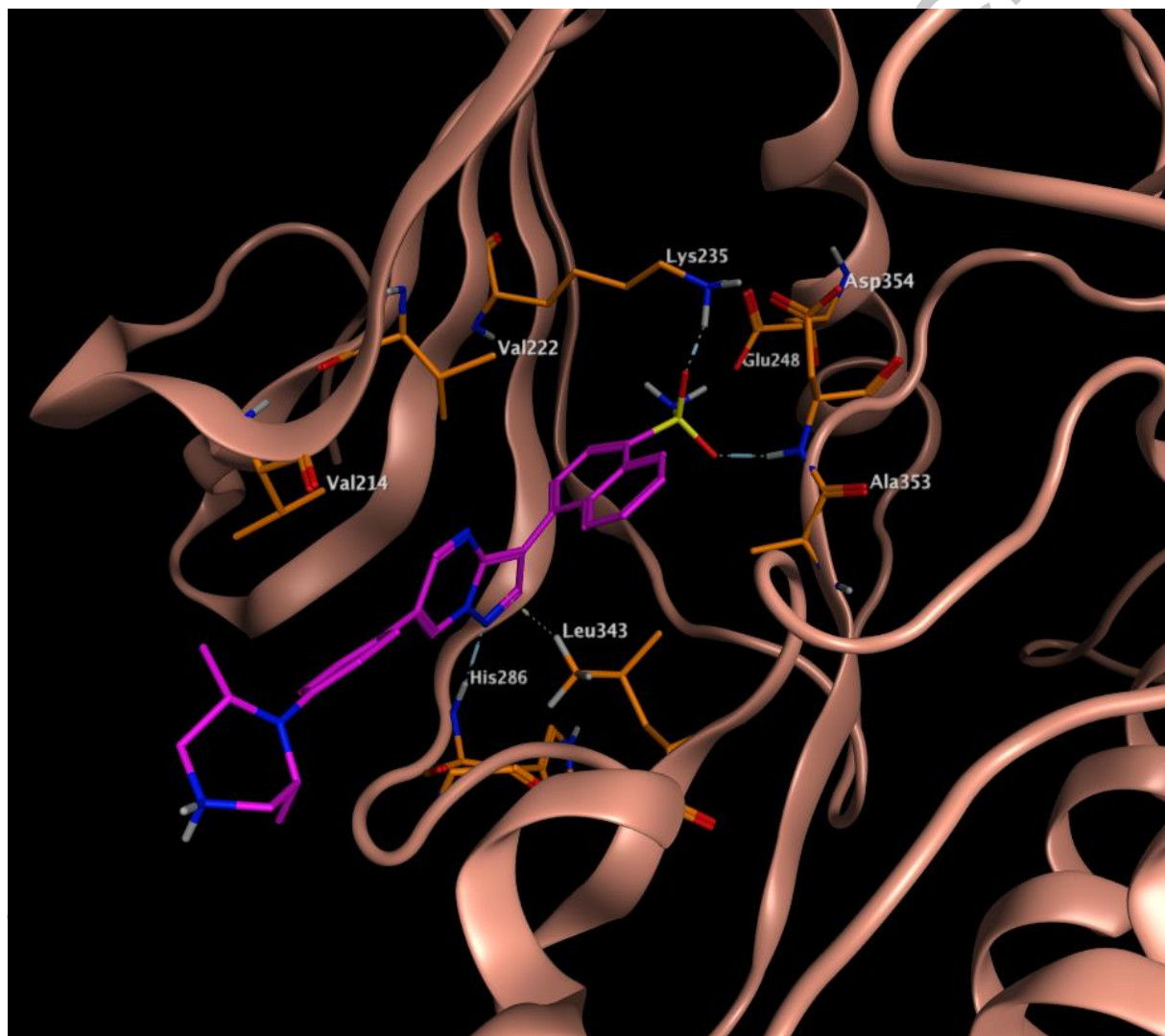

Figure 2. Computational modeling of the interaction of **7** with ALK2.
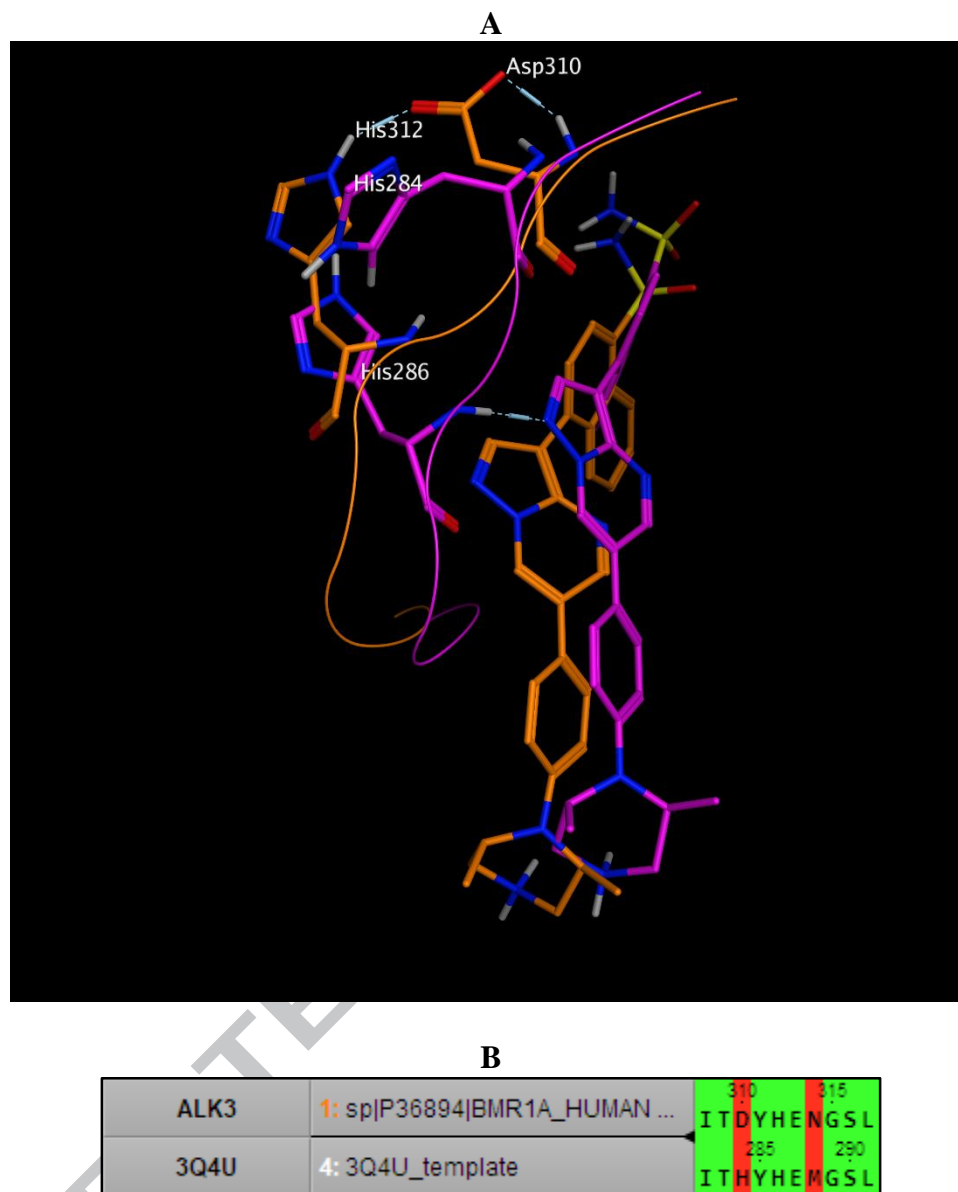
A

B

Figure 3. Compound **7** modeled into the ALK2 (pink) and ALK3 (orange) binding pockets. **A.** The hinge backbones for ALK2 and ALK3 are shown as a lines. Hinge residues His 284, 286 (ALK2) and Asp310, His312 (ALK3) are explicitly shown. **B.** ALK2-ALK3 hinge region sequence alignment
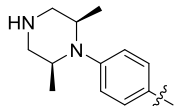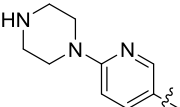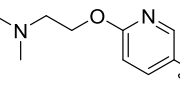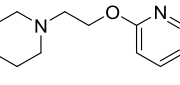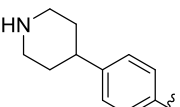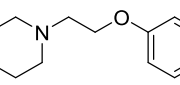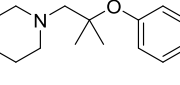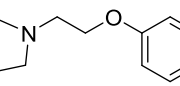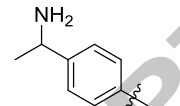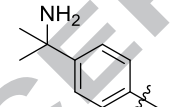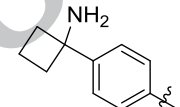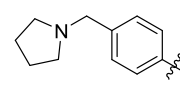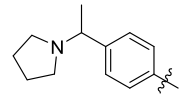
Although **7** demonstrated promising potency and selectivity for ALK2, early in-house ADME profiling showed this compound had poor permeability, as measured in PAMPA (5.5×10^{-6} cm/s) and aqueous solubility (1.8 μg/ml at pH 7.4). To further improve both ALK2 potency and ADME properties, more comprehensive SAR efforts were carried out focusing on changes to the 6-position of the pyrazolo[1,5-a]pyrimidine core via compounds **12-23**. Each new analog was assessed not only for its inhibition of ALK2 and ALK3, but also for its early ADME parameters, including RLM stability, PAMPA permeability, and aqueous solubility at pH 7.4.

8

As shown in Table 2, replacing the phenyl ring with a pyridinyl linker resulted in a >20-fold decreased ALK2 inhibitory activity as exemplified by analogs **12**, **13** and **14**, although **14** showed significant improvement in PAMPA permeability with the more lipophilic 2-(piperidinyl)ethoxy moiety. Analog **15** with a phenylpiperidinyl ring showed modest improvement in PAMPA permeability, but was only ~5-fold less potent (IC_{50}= 93 nM) than **7**, suggesting that the phenyl linkage might reinstate potency for ALK2. Analogs with a 2-(piperidinyl)ethoxy chain such as **16** and **17** exhibited IC_{50} values < 100 nM for ALK2 with significantly improved PAMPA permeability, although **17** showed shorter half-life in RLM compared to **16**, which might be derived from favorable cleavage of the tertiary C-O bond. Analog **18** with a five-membered pyrrolidinyl ring showed ~10-fold improvement of aqueous solubility compared to **16** and retained good RLM stability and PAMPA permeability. Despite its optimized ADME properties, **18** was still ~3-fold less potent than LDN-193189 for ALK2 thus more optimization at the 6-position of the core was pursued. Gratifyingly, benzylic amine analogs such as **19**-**21** showed improved inhibitory potency for ALK2 compared to **18**, although their PAMPA permeability decreased dramatically. This might be attributed to the polar primary amine functionality. Incorporation of a pyrrolidinyl ring to give analog **22** not only maintained similar ALK2 inhibitory activity as **19**, but regained PAMPA permeability (467×10^{-6} cm/s). Finally, adding a methyl group at the benzylic position culminated in the discovery of compound **23** that was not only ~2-fold more potent than **7**, but also showed >700-fold selectivity against ALK3. It also exhibited amenable ADME properties as indicated by its excellent PAMPA permeability, acceptable RLM stability ($t_{1/2}$= 22.8 min) and aqueous solubility at pH 7.4 (7 μg/ml or 14 μM), which is ~4-fold increase compared to **7** (1.8 μg/mL at pH 7.4).

Table 2. ALK2 and ALK3 inhibitory activity, RLM stability, PAMPA permeability and aqueous solubility of **7**-**23**, which represent changes to the 6-position of the pyrazolo[1,5-a]pyrimidine.
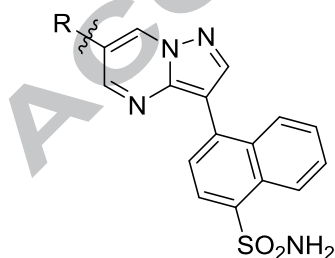
Compd	R	ALK2 (IC_{50}, nM)	ALK3 (IC_{50}, nM)	Selectivity (-fold)	RLM $t_{1/2}$ (min)	PAMPA ($\times 10^{-6}$ cm/s)	Aq. sol. (μg/mL)

9

#	Structure						
7		19	3466	182.4	>30	5.5	1.8
12		422	>10,000	NA	>30	8.3	1.4
13		1026	>10,000	NA	9.4	8.8	<1
14		738	>10,000	NA	20.9	364.7	<1
15		93	>10,000	NA	>30	78.6	<1
16		63	>10,000	NA	>30	481.5	3.2
17		47	>10,000	NA	6.1	1920.5	<1
18		48	>10,000	NA	>30	317	33
19		25	12830	513.2	ND	14.2	7.6
20		29	>10,000	NA	>30	9.4	10.6
21		16	8195	512.2	ND	ND	<1
22		27	>10,000	NA	21.9	467	8
23		9	6439	715.4	22.8	1116.0	7.0

To better understand the enzyme selectivity of **23**, it was profiled against other BMP type 1 receptor kinases (ALK1, ALK4, ALK5 and ALK6) and four upstream BMP type 2 receptor

10

kinases (ACVR2A, ACVR2B, BMPR1 and TGFβR2)[25] (Table 3). The results indicated **23** was highly selective among both BMP type 1 and 2 receptor kinases with the exception of ALK1 (IC_{50}= 51 nM), which was not surprising considering the high sequence homology in the ATP binding pockets of ALK1 and ALK2.[26] In addition, LDN-193189, **7** and **23** were evaluated for their cellular activity through measuring their inhibition of BMP6 (an ALK2 ligand) induced transcriptional activity (BRE-Luciferase) in C2C12 cells as previously reported.[27] While compound **23** (EC_{50} = 8 nM) had similar cellular activity as LDN-193189 (EC_{50} = 14 nM), compound **23** was about 11-fold more potent than compound **7** (EC_{50} = 91 nM). It should be noted that **23**'s high selectivity against ALK5 (also called TGFβR1) and TGFβR2 might be advantageous since it is well known that chronic inhibition of TGFβ-signaling is associated with immunosuppression, physeal hypertrophy and cardiac valvulopathy.[28-29] Also kinome-wide profiling of **21**, which is structurally similar to **23**, at 1 μM found only five non-BMP receptor kinases (ARK5, DDR1, MAP4K5, RIPK2 and TNIK) out of 252 kinases with >80% inhibition (for the detailed results, see Supplementary Material), further showcasing the high selectivity of this class of ALK2 inhibitors versus other kinases.

Table 3. Enzymatic activities of analog **23** for BMP type 1 and type 2 receptor kinases (IC_{50}, nM).

Enzyme	ALK1	ALK4	ALK5	ALK6	ACVR2A	ACVR2B	BMPR2	TGFβR2
Compd 23	51	18330	18650	13140	2370	3130	>10,000	698

Pharmacokinetic parameters of **23** were determined in C57BL/6 mice after single intraveneous (IV) and oral (PO) administration of 3 mg/kg for each route (Table 4). This analog showed a relative low plasma clearance (CLp) of 16 mL/min/kg and a moderate half-life of 3-4 hours. It appears that the compound distributed extensively to the tissues based on its large steady-state volume of distribution (V_{dss} = 4.6 L/kg). The oral bioavailability (%F) was 24%.

Table 4. In vivo pharmacokinetic parameters of **23** in mice.

Pharmacokinetic Parameters of **23** in C57BL/6 Mice (3 mg/kg)		
Route	IV	PO
$AUC_{0\to\infty}$ (hr•ng/mL)	3220	782
$t_{1/2}$ (h)	3.5	4.3
C_{max} (ng/mL)		67
CL (mL/min/kg)	16	
V_{dss} (L/kg)	4.6	
%F		24

In summary, we discovered a novel class of selective ALK2 inhibitors with 4-(sulfamoyl)naphthyl as the pendant substituent at the 3-position of the pyrazolo[1,5-a]pyrimidine core. Compound **23** not only showed excellent ALK2 inhibitory activity, which was comparable to LDN-193189, but excellent selectivity against other kinases including BMP type 1 and 2

11

receptor kinases. Compound **23** also showed acceptable in vivo pharmacokinetics therefore positioning this class of ALK2 inhibitors for further development towards the treatment of FOP.

Acknowledgments

References and notes

1. Buyse G, Silberstein J, Goemans N, Casaer P. Fibrodysplasia ossificans progressiva: still turning into wood after 300 years? *Eur. J. Pediatr*. 1995; 275: 694-699.
2. Shore EM, Kaplan FS. Insights from a rare genetic disorder of extra-skeletal bone formation, fibrodysplasia ossificans progressiva (FOP). *Bone*. 2008; 43: 427-433.
3. Kaplan FS, LeMerrer M, Glaser DL, Pignolo RJ, Goldsby RE, Kitterman JA Groppe J, Shore EM. Fibrodysplasia ossificans progressiva. *Best Pract. Res. Clin. Rheumatol*. 2008; 22:191-205.
4. Kaplan FS, Glaser DL, Pignolo RJ, Shore EM. A new era for fibrodysplasia ossificans progressiva: a druggable target for the second skeleton. *Expert Opin. Biol. Ther.* 2007; 7: 705-712.
5. Shore EM, Xu M, Feldman GJ, Fenstermacher DA, Cho TJ, Choi IH, Connor JM, Delai P, Glaser DL, LeMerrer M, Morhart R, Rogers JG, Smith R, Triffitt JT, Urtizberea JA, Zasloff M, Brown MA, Kaplan FS. A recurrent mutation in the BMP type I receptor ACVR1 causes inherited and sporadic fibrodysplasia ossificans progressiva. *Nat. Genet.* 2006; 38: 525-527.
6. Hatsell SJ, Idone V, Wolken DM, Huang L, Kim HJ, Wang L, Wen X, Nannuru KC, Jimenez J, Xie L, Das N, Makhoul G, Chernomorsky R, D'Ambrosio D, Corpina RA, Schoenherr CJ, Feeley K, Yu PB, Yancopoulos GD, Murphy AJ, Economides AN. ACVR1R206H receptor mutation causes fibrodysplasia ossificans progressiva by imparting responsiveness to activin A. *Sci Transl Med.* 2015; 303ra137.
7. Hino K, Ikeya M, Horigome K, Matsumoto Y, Ebise H, Nishio M, Sekiguchi K, Shibata M, Nagata S, Matsuda S, Toguchida J. Neofunction of ACVR1 in fibrodysplasia ossificans progressiva. *Proc. Natl. Acad. Sci.* 2015; 112: 15438-15443.
8. Regeneron Shares Updates on its Ongoing FOP Research Program, http://www.ifopa.org/regeneron_shares_updates_on_its_ongoing_fop_research_program.
9. Chakkalakal SA, Uchibe K, Convente MR, Zhang D, Economides AN, Kaplan FS, Pacifici M, Iwamoto M, Shore EM. Palovarotene Inhibits Heterotopic Ossification and Maintains Limb Mobility and Growth in Mice With the Human ACVR1(R206H) Fibrodysplasia Ossificans Progressiva (FOP) Mutation. *J. Bone Miner.Res.* 2016; 31: 1666-1675.
10. Hino K, Horigome K, Nishio M, Komura S, Nagata S, Zhao C, Jin Y, Kawakami K, Yamada Y, Ohta A, Toguchida J, Ikeya M. Activin-A enhances mTOR signaling to
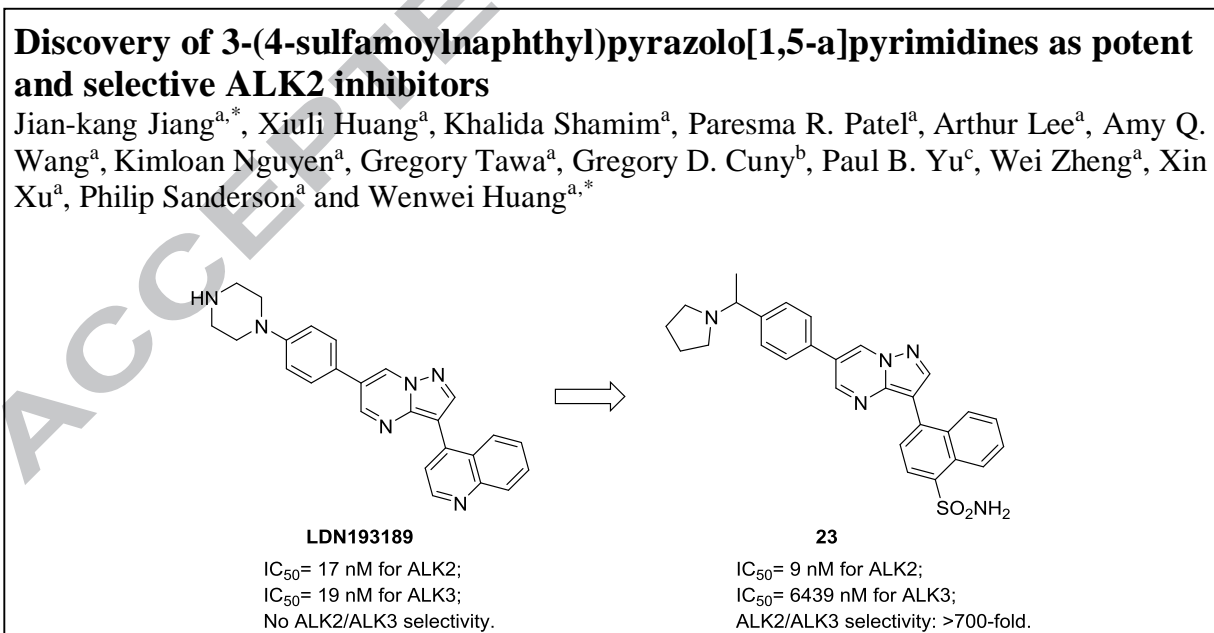
promote aberrant chondrogenesis in fibrodysplasia ossificans progressiva. *J. Clin. Invest.* 2017; 127: 3339-3352.

11. Kaplan FS, Zeitlin L, Dunn SP, Benor S, Hagin D, Al Mukaddam M, Pignolo RJ. Acute and chronic rapamycin use in patients with Fibrodysplasia Ossificans Progressiva: A report of two cases. *Bone*. 2018, 109: 281-284

12. Cuny GD, Yu PB, Laha JK, Xing X, Liu JF, Lai CS, Deng DY, Sachidanandan C, Bloch KD, Peterson RT. Structure-activity relationship study of bone morphogenetic protein (BMP) signaling inhibitors. *Bioorg Med Chem Lett.* 2008; 18: 4388-4392.

13. Yu PB, Deng DY, Lai CS, Hong CC, Cuny GD, Bouxsein ML, Hong DW, McManus PM, Katagiri T, Sachidanandan C, Kamiya N, Fukuda T, Mishina Y, Peterson RT, Bloch KD. BMP type I receptor inhibition reduces heterotopic ossification. *Nat. Med.* 2008; 14: 1363-1369.

14. Hao J, Ho JN, Lewis JA, Karim KA, Daniels RN, Gentry PR, Hopkins CR, Lindsley CW, Hong CC. In vivo structure-activity relationship study of dorsomorphin analogues identifies selective VEGF and BMP inhibitors. *ACS Chem. Biol.* 2010; 5: 245-253.

15. Hamasaki M, Hashizume Y, Yamada Y, Katayama T, Hohjoh H, Fusaki N, Nakashima Y, Furuya H, Haga N, Takami Y, Era T. Pathogenic mutation of ALK2 inhibits induced pluripotent stem cell reprogramming and maintenance: mechanisms of reprogramming and strategy for drug identification. *Stem Cells*, 2012; 30: 2437-2449.

16. Engers DW, Frist AY, Lindsley CW, Hong CC, Hopkins CR. Synthesis and structure-activity relationships of a novel and selective bone morphogenetic protein receptor (BMP) inhibitor derived from the pyrazolo[1.5-a]pyrimidine scaffold of dorsomorphin: the discovery of ML347 as an ALK2 versus ALK3 selective MLPCN probe. *Bioorg. Med. Chem. Lett.* 2013; 23: 3248-3252.

17. Mohedas AH, Xing X, Armstrong KA, Bullock AN, Cuny GD, Yu PB. Development of an ALK2-biased BMP type I receptor kinase inhibitor. *ACS Chem. Biol.* **2013**, *8*, 1291-1302.

18. Sanvitale CE, Kerr G, Chaikuad A, Ramel MC, Mohedas AH, Reichert S, Wang Y, Triffitt JT, Cuny GD, Yu PB, Hill CS, Bullock AN. A new class of small molecule inhibitor of BMP signaling. *PLoS One*. 2013; 8: e62721.

19. Kim M, Choi O, Pyo S, Choi SU, Park CH. Identification of novel ALK2 inhibitors and their effect on cancer cells. *Biochem. Biophys. Res. Commun.* 2017; 492: 121-127.

20. Dorsch, D.; Jonczyk, A.; Krier, M. WO2016165808A1.

21. Fleming PE, Hondous BL, Kim JL, Waetzig J, Williams B, Wilson D, Wilson KJ. WO2017181117A1.

22. Hopkins CR. Inhibitors of the bone morphogenetic protein (BMP) signaling pathway: a patent review (2008-2015). *Expert Opin. Ther. Pat.* **2017**, *26*, 1115.

23. Li J, Arista L, Babu S, Bain J, Cui K, Dillon MP, Lattmann R, Liao L, Lizos D, Ramos R, Stiefl N J, Ullrich T, Usselmann P, Wang X, Waykole LM, Weiler S, Zhang Y, Zhou Y, Zhu T. WO2018014829A1.

24. Williams E, Bullock AN. Structural basis for the potent and selective binding of LDN-212854 to the BMP receptor kinase ALK2. *Bone*, 2018; 109: 251-258.

25. The IC_{50} values of analog **23** for other BMP type 1 receptors were measured in the same manner as ALK2 or ALK3 by using 10 μM ATP. The IC50 values of **23** for BMP type 2 receptors were measured by Life Technologies, a subdivision of ThermoFisher using LanthaScreen[TM] kinase activity assay.

26. Kerr G, Sheldon H, Chaikuad A, Alfano I, von Delft F, Bullock AN, Harris AL. A small molecule targeting ALK1 prevents Notch cooperativity and inhibits functional angiogenesis. *Angiogenesis*, 2015; 18: 209-217.

27. Mohedas AH, Wang Y, Sanvitale CE, Canning P, Choi S, Xing X, Bullock AN, Cuny GD, Yu PB. Structure-activity relationship of 3,5-diaryl-2-aminopyridine ALK2 inhibitors reveals unaltered binding affinity for fibrodysplasia ossificans progressiva causing mutants. *J. Med. Chem.* 2014; 57: 7900-7915.

28. Shi Y, Massagué J. Mechanisms of TGF-beta signaling from cell membrane to the nucleus. *Cell*, 2003; 113: 685-700.

29. Gueorguieva I, Cleverly AL, Stauber A, Sada Pillay N, Rodon JA, Miles PA, Yingling JM, Lahn MM. Defining a therapeutic window for the novel TGF-β inhibitor LY2157299 monohydrate based on a pharmacokinetic/pharmacodynamic model. *Br. J. Clin. Pharmacol.* 2014; 77: 796-807.

Supplementary Material

Supplementary material includes the experimental procedure for the measurement of IC$_{50}$ values for ALK1-6, the method of computer modeling of interaction of ALK2 and ALK3 binding with analog **7**, the synthetic procedures and spectral characterization of all analogs (**1-23**) and the profiling of the inhibition of analog **21** against 252 kinases at 1 µM concentration.

Graphical Abstract

Discovery of 3-(4-sulfamoylnaphthyl)pyrazolo[1,5-a]pyrimidines as potent and selective ALK2 inhibitors

Jian-kang Jiang[a,*], Xiuli Huang[a], Khalida Shamim[a], Paresma R. Patel[a], Arthur Lee[a], Amy Q. Wang[a], Kimloan Nguyen[a], Gregory Tawa[a], Gregory D. Cuny[b], Paul B. Yu[c], Wei Zheng[a], Xin Xu[a], Philip Sanderson[a] and Wenwei Huang[a,*]

LDN193189
IC$_{50}$= 17 nM for ALK2;
IC$_{50}$= 19 nM for ALK3;
No ALK2/ALK3 selectivity.

23
IC$_{50}$= 9 nM for ALK2;
IC$_{50}$= 6439 nM for ALK3;
ALK2/ALK3 selectivity: >700-fold.

14

- Identification of a novel class of 4-sulfamoylnaphthyl series ALK2 inhibitor

- Excellent selectivity for ALK2 over ALK3 with additional overall kinome selectivity

- Key distinctive features identified in the ALK3 homology model to explain ALK2 *vs* ALK3 selectivity